E. Tescaroli, M. Belan
An Original Pitot-Static Probe Design for Subsonic Boundary Layer Investigation
Measurement Science & Technology, Vol. 32, N. 6, 2021, 065301 (7 pages)
doi:10.1088/1361-6501/abf057

An original Pitot-static probe design for subsonic boundary layer investigation

E Tescaroli and M Belan

Politecnico di Milano, Department of Aerospace Science and Technology, Via La Masa 34, 20156 Milano, IT

E-mail: marco.belan@polimi.it

Abstract. This work presents a Pitot-static probe designed and developed to help in some boundary layer measurements, as for instance when average velocity profiles are required around models already available for wind tunnel tests but not provided with static pressure taps. The probe reads both total and static pressures at the desired location and by traversing it through the boundary layer leads to the desired velocity measurements on the body under test, without having to rebuild the model and without using more expensive and complicated techniques. The probe is presented by describing its geometry in detail and completing the information by the relevant operating instructions. The probe response is then characterized by reporting its directional sensitivity and a validation for a standard test case. The specific probe presented here is suitable for a certain range of boundary layer thicknesses, however the design can be easily scaled to different ranges.

Keywords: Pitot-static probe, boundary layer, probe calibration

Submitted to: *Meas. Sci. Technol.*

1. Introduction

By simply relying on pairwise pressure readings, the pressure-based technique certainly classifies as one of the simplest fluid-dynamics investigation techniques to acquire average velocity profiles in a flow field. Indeed, it can be promptly shown [1] that incompressible, steady and isentropic flows satisfy the Bernoulli relation:

$$P_0 = P + \frac{1}{2}\rho U^2 \tag{1}$$

which returns the flow velocity U at a certain point in space once the local values of total P_0 and static P pressures are provided. The total pressure can be measured using a Pitot tube, while either static probes or wall tappings can be adopted for static pressure reading. Assuming an ideal gas to be the fluid under exam, its density ρ is computed from the equation of state:

$$\frac{P}{\rho} = RT \tag{2}$$

starting from the values of P, T and R, i.e. the pressure, temperature and specific gas constant in the measuring location. If needed, moisture effect can be accounted for introducing a humidity correction [2]. Equation (1) can also be used in the case of measurements on a liquid of known density.

Traditional Pitot-static probe design combines total and static probes in a rather compact shape capable of providing accurate simultaneous pressure readings in closely located positions. Owing to these characteristics, it constitutes a *de-facto* standard solution for quick free-flows velocity evaluations in fluid dynamics experiments. Despite the undeniable advantage of having a unique sensor, this solution suffers from the higher footprint necessary to hold both devices in a single body. This is particularly penalizing in near-wall investigations, where minimizing the intrusive effects is crucial for the reliability of the measurements and can only be guaranteed by sensors with dimensions comparable to the local length scales of the flow. In fact, in boundary layer (BL) velocity investigations the pressure reading techniques generally require the use of miniaturized Pitot probes, avoiding the larger Pitot-static probes.

As is well known, other techniques are available for BL velocity measurements, e.g. laser-Doppler velocimetry (LDV), micro Particle Image Velocimetry (μ-PIV) and hot-wire anemometry (HWA), all capable of ensuring great levels of accuracy if properly set. LDV is highly accurate and gives average as well as time resolved quantities, however it is an expensive technique and requires a careful optical alignment for each definite setup. μ-PIV returns complete velocity fields with good accuracy but generally lower with respect to LDV; it is already expensive when average values are required, and the cost is even higher for time-resolved quantities. The lower cost solutions are highly appealing, among these HWA gives time-resolved measurements with a wide frequency response. However these techniques are not drawbacks-free, for instance HWA requires repetitive calibrations and the hot-wire probe positioning with respect to the wall is a major issue. All the techniques above intrinsically involve a considerable level of complexity reflecting into the need for specific apparatuses and highly qualified personnel. On the other hand, when the aim is to measure only average values, a pressure reading system based on a Pitot probe is easier to implement, robust and less expensive, moreover it is based on a linear relationship between pressure and output signal. A good accuracy can be obtained by choosing suitable transducers.

For Pitot probes, a key parameter in BL measurements is the spatial resolution. This is essentially related to the probe diameter, and for Pitot-static devices it is generally poor because of their coaxial pipes structure. The resolution of miniaturized Pitot probes instead can be much better thanks to their lower diameters, at the price of a larger response time for the measurement system. Probes of diameter well below 1 mm are reported in literature, for example a 0.2mm cylindrical head is used in [3], and it is possible to bring the probe size below 0.1mm along the wall normal direction by adopting a flattened shape [1].

The technique here presented is based on a variant to the classical Pitot-static design offering the possibility of retaining co-located total and static pressure measurements

in a boundary layer flow without sacrificing the spatial resolution and reducing the intrusive effects to a minimum degree. The device itself was originally thought to tackle the necessity of measuring velocities in proximity of complex flow control electrohydrodynamic devices on a wind tunnel model where wall tappings were difficult to introduce [4, 5], without giving up the versatility, simplicity and the affordability offered by pressure probes. More generally, the field of use can be extended to BL measurements on models or surfaces not provided with pressure taps (for example, wind tunnel models already built for force measurements), avoiding the reconstruction of new versions of the same models.

2. Description of the instrument and procedure of operation

In order to provide guidelines to correctly size and use the probe, some considerations that originated the instrument design are discussed in this section. In what follows, it is presented a probe with definite size and proportions, designed to work on a given range of BL thicknesses; however, the same kind of probe with different dimensions can be realized in a similar way, by tailoring it to the flow under examination.

2.1. Design guidelines

The probe is presented in figure 1, with dimensions specified in table 1. Two pneumatically independent yet mechanically joined parts are identifiable: the total-head probe (or Pitot tube), with its nose protruding from the front of the device, and the static probe, recognizable by the surface tappings positioned further downstream. Separate total and static pressures are read on the opposite end of the device from port A and B, respectively. The uncertainty on the total head diameter is $\pm 10\mu$m as specified by the tube manufacturer, for the other dimensions in table 1 the uncertainty is $\pm 25\mu$m.

Table 1. List of main dimensions adopted for the probe in figure 1.

d_1	0.4	mm	$d_{1,int}$	0.24	mm
d_2	1.0	mm	ℓ_1	18.0	mm
d_3	2.5	mm	ℓ_2	16.0	mm
d_4	0.7	mm	ℓ_3	4.0	mm

In the specimen shown here the Pitot tube is made of a cylindrical square-ended metal tube with its head exposed to the flow, whereas the rear part enters the static probe guaranteeing in this manner a mechanical protection against undesirable deformations. The inner tube remains coaxial to the external one for its whole length, leaving a small gap in between to ensure proper functioning of the static probe. All joints between consecutive parts are sealed with cyanoacrylate glue and accurately sanded to remove edges and imperfections and to provide slenderness to the build. Burrs left after drilling or puncturing the surface of the tube were carefully sanded and cleaned

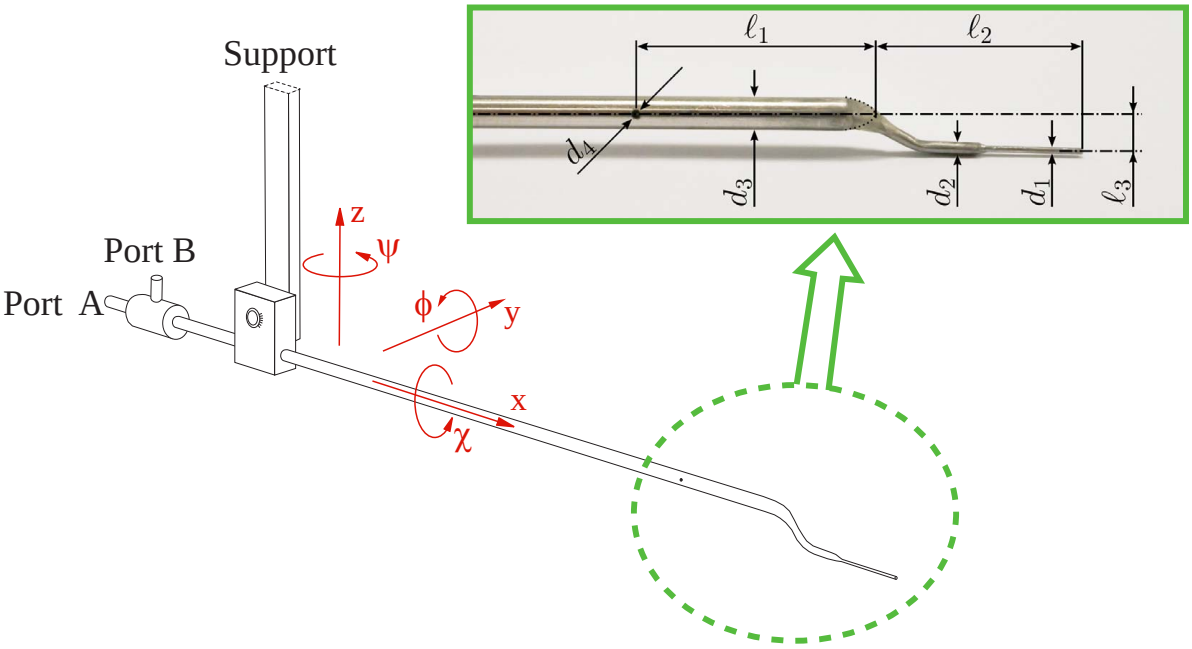

Figure 1. Sketch and photograph of the presented probe, with details of the fore portion and body reference frame.

as well, verifying the final result with a microscope. Pressure tests on the final product performed in a water vessel helped verifying the absence of improper air leakages from the sealings.

Sizing the total-head probe requires a preliminary examination of the flow behaviour in proximity of the surface. Valuable information comes from an a priori estimate of the expected thickness magnitude, whether this knowledge comes from preliminary numerical simulations or literature on similar flows. Intuitively, the head diameter should be comparable with the viscous length scale δ_ν in the region of interest. In fact, a diameter of few δ_ν would not only allow to resolve the velocity profile closer to the wall, but also to have a higher spatial resolution because of the small frontal area of the tube. Further, it may help reducing the intrusive effects of the instrument into the flow. Conversely, the smaller the tube diameter, the slower the time response and considering that measurements need to be averaged over a time window wide enough to guarantee convergence of the reading, having a poor frequency response might not be recommended. Secondarily, the viscous length scale can be very small when measured in physical coordinates, even in the order of μm, therefore real-world feasibility from the construction standpoint should be accounted for. The final dimensions and proportions for the probe should be selected as the best tradeoff amongst these contrasting effects, aiming to an adequate spatial resolution without suffering from excessively long response times. For the case where this probe was first introduced [4, 5], preliminary estimations of the flow characteristics from literature consultation [6] and further refinement by numerical simulations gave a viscous length scale in the region of interest ranging from 10 to 20 μm. With an outer diameter $d_1 = 0.4$ mm and a inner-to-outer diameter ratio

$\theta = d_{1,int}/d_1 = 0.6$, the presented design solution allowed to cover the great majority of the BL vertical extension by starting the measurements in proximity of the lower end of the buffer region, i.e. $y^+ = y/\delta_\nu \approx 50$, while preserving the sturdiness of the build.

Sizing of static probe is instead far less critical. The diameter of the tube has to be selected to internally accommodate the total-head tube without losing sight of the larger flow interferences caused by the larger dimensions. Tappings need to be placed well downstream of the tip and upstream of the support to be unaffected by their presence, safe distances in literature are typically in the order of 6 diameters from the tip and 15 from the stem. Generally, the use of multiple holes uniformly distributed around the tube circumference at a given position is recommended to balance the effects of excessive lateral velocity components. On this design, the use of two horizontally leveled holes is suggested in order to measure at the same wall distance. The requirement of small diameter orifices with respect to the local BL scale is easy to fulfill by using the δ_{99} thickness as a term of comparison. As a reference, the δ_{99} estimate around a NACA 0015 airfoil model in the cited dataset [4, 5] varied between 1.2 and 4.5 mm depending on the location on the model, thus an offset $l_3 = 4.0$ mm and a hole diameter of 0.7 mm were selected.

The vertical (wall-normal) offset ℓ_3 between total and static holes introduced by the curvings in the total-head tube is specifically thought to exploit the uniformity of the static pressure across the BL at first order approximation, implying that reliable information on the value at wall can be captured at or just outside the edge of the BL. The horizontal (streamwise) offset $\ell_1 + \ell_2$ between total and static holes instead is managed by a suitable shift of the probe, as explained in the next section.

2.2. Operating instructions for boundary layer measurements

A two-step procedure - illustrated in figure 2 - is prescribed for BL measurements at each point of interest:

(1) Starting with the tip in contact with the model surface at point Q, acquire total-pressure data by traversing the BL in height (z-direction) with a predetermined step size Δz ensuring to correctly resolve the local velocity profile (figure 2, top).

(2) Shift the probe forward by the amount $\Delta x_{t-s} = \ell_1 + \ell_2$, i.e. the horizontal distance between tip and static tappings, in order to align the static holes to the position Q previously occupied by the tip and then lower the probe close to the wall. Acquire the static pressure data through the static holes that lie in the outer region of the BL (figure 2, bottom), at a z position not critical for this reading.

Total and static pressure readings are acquired using separate differential pressure transducers referring to a common desired quantity, e.g. ambient pressure, their difference is then used in (1) to compute the velocity. Since positioning is fundamental, the use of an high accuracy positioning system is recommended. Determination of the initial position ($z = z_Q = 0$ mm) can be accomplished by carefully approaching the surface from the top and using the mirrored image method (or equivalent) to verify the

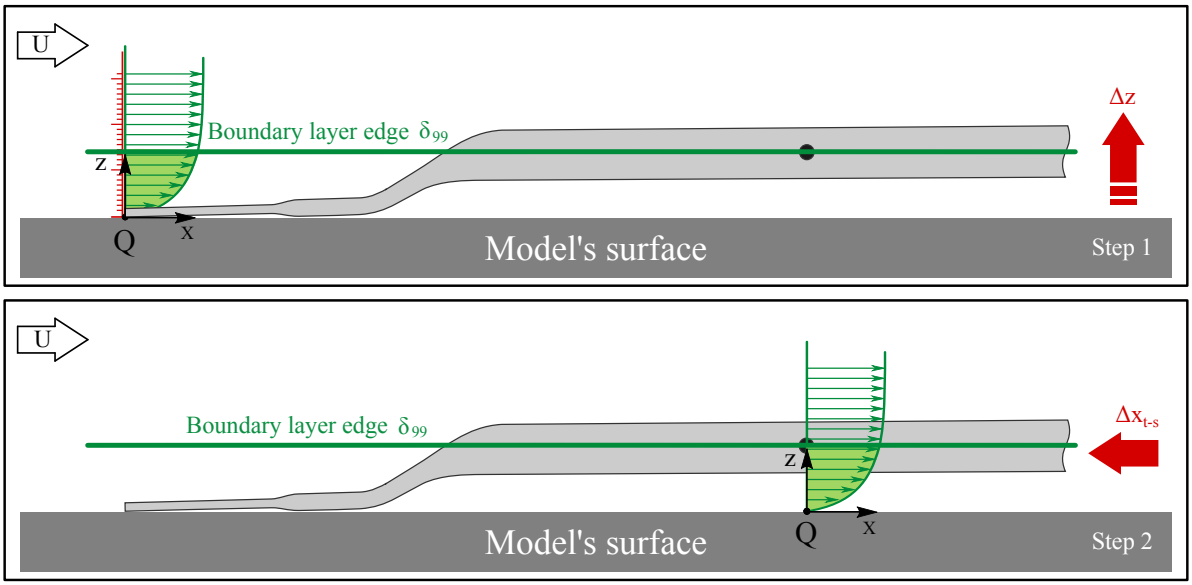

Figure 2. Schematic for the two-step positioning of the probe above the model surface during BL investigation (wall reference frame). The probe reads total and static pressures at the same point Q moving along the surface in two steps.

contact of the probe tip with the surface. On a flat surface, the probe can be slightly tilted as in figure 2 (in the order of 2°) to ensure that the tip is touching the surface properly, whilst this adjustment is generally not required on a convex surface. The sketches in figure 1 and 2 represent also a typical application case: the probe is held above a model or surface and the supporting system is used to traverse the probe along the x and z axes near the wall.

3. Validation and discussion

This section first presents a sensitivity assessment of this design to misalignments with respect to the main flow direction. This evaluation is then complemented by the outcome of a standard calibration test aimed at verifying the effectiveness and reliability of the proposed design in reconstructing BL average velocity profiles.

Experiments were held in the low-turbulence wind tunnel "Sergio de Ponte" at Politecnico di Milano, a facility certified for anemometers calibration with maximum airspeed 55 m/s, angular deviation of the streamlines lower than 0.1° and turbulence level lower than 0.3%. The tunnel is of the closed return type with rectangular section of aspect ratio 3:2, held constant along the whole circuit. The area ratio of the contraction is 7:1. The test section is closed, with nominal cross-section 1×1.5 m and a length of 3 m. The actual cross-section is slowly growing thanks to the diverging walls (0.2°), adopted to allow the boundary layer thickening and avoid a longitudinal pressure gradient. A breather downstream of the test section with removable coverings on its 4 sides and an auxiliary tangential blower installed close to the first corner permit an accurate control of the pressure in the test section, which can be equalized with the atmospheric

pressure or also put in overpressure. Equalizing the pressure with the external one avoids possible air bleeding into the tunnel through imperfect sealings of the supports/cables feedthroughs, and minimizes boundary layer disturbances. This setup maintains along the test section a very low pressure variation, that can be quantified by means of the pressure coefficient

$$c_P = \frac{P - P_i}{\frac{1}{2}\rho U_i^2}, \tag{3}$$

referred to the inlet pressure and velocity P_i, U_i. The resulting value is $c_P = 0 \pm 0.025$, assumed as condition of zero pressure gradient for the present tests. In literature it is possible to find even better conditions, however they are typically obtained in facilities purposely designed for boundary layer studies [3, 7, 8].

3.1. Effects of geometry on directional sensitivity

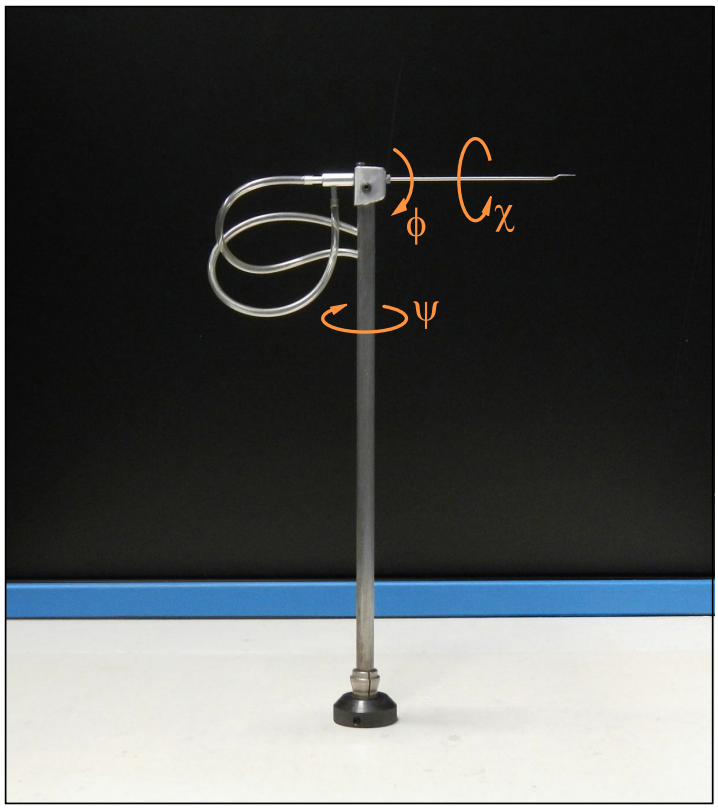

Figure 3. Setup for angular sensitivity measurements. Reference system as in figure 1.

To characterize the probe behaviour relative to roll, pitch, yaw rotations with angles χ, ϕ, ψ respectively as in figure 1, a classical freestream directional sensitivity calibration was performed. The directional sensitivity setup is shown in figure 3, with the same reference system of figure 1, however in this case the vertical support is mounted on the tunnel floor and aligned normally to the tunnel centerline (not to the floor, which is slightly inclined as explained in the tunnel description above). The

yaw ψ is set by a rotary system driven by a stepper motor below the tunnel floor, with positioning accuracy of $\pm 0.005°$. Accounting for the mechanical tolerances and for the small crossflow of the wind tunnel, the resulting uncertainty of yaw ψ is $\pm 0.1°$. Pitch ϕ and roll χ are manually set by acting on the probe joint, which is locked at the desired position after reading the direction by a inclination sensor, coupled to the probe body with a mechanical adapter. The positioning accuracy of the sensor is $\pm 0.02°$, however the final accuracy owing to tunnel crossflow and manual locking is $\pm 0.2°$. For this test the horizontal translation of the probe described in the procedure for wall measurements (§2.2) is not needed, thus the pressure lines are connected to a single differential transducer with Full Scale 100 Pa and 0.1% FS accuracy, coupled with a 16-bit acquisition module collecting data at a sampling frequency of 1 kHz for a time window of several seconds to ensure convergence. The airspeed in the wind tunnel is 10 m/s.

The calibration consists in determining the variations in the pressure coefficient c_{Pd}, defined as the measured-to-reference dynamic pressure ratio

$$c_{Pd} = \frac{P_{\text{dyn,meas}}}{P_{\text{dyn,ref}}} \tag{4}$$

for several combinations of the mentioned angles. This coefficient permits to evaluate the deviation with respect to the wind tunnel value $P_{\text{dyn,ref}}$, kept fixed during the entire test campaign. The overall accuracy of the resulting c_{Pd} values is in the order of $\pm 0.25\%$. For the presented design the response was found to be independent of the roll χ and

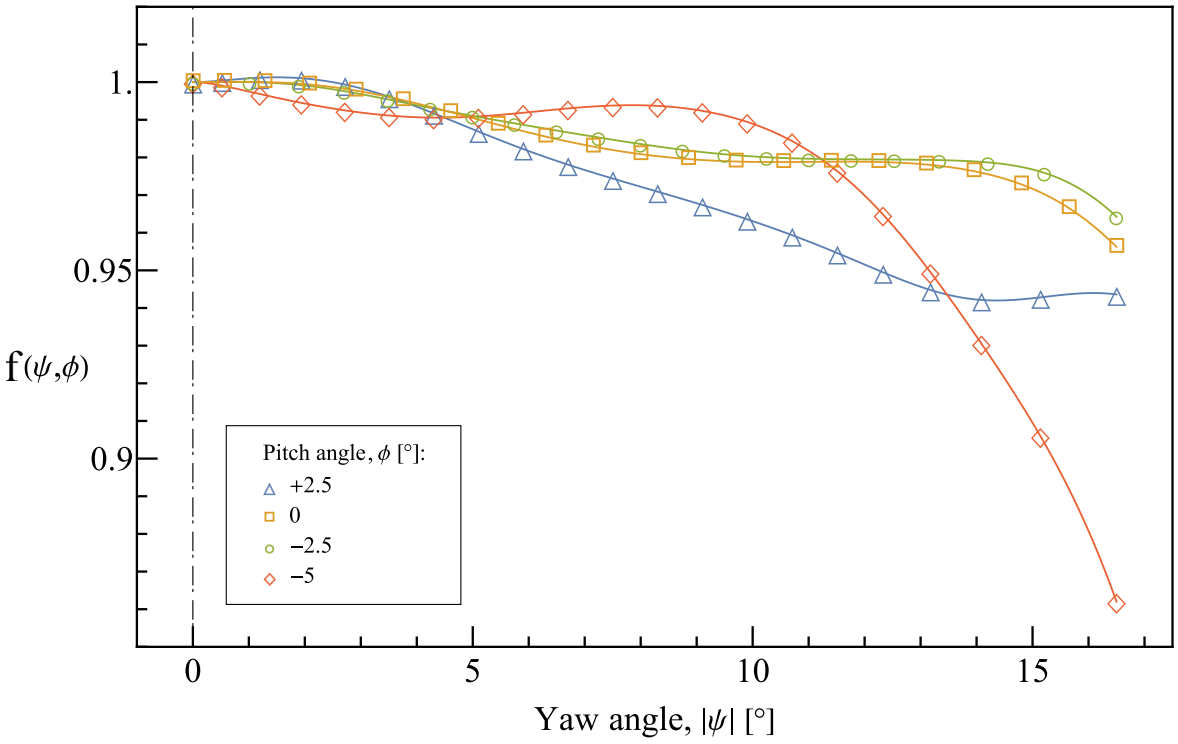

Figure 4. Probe sensitivity to variations in pitch and yaw angles, the relevant offset is reported in table 2.

determined by yaw ψ and pitch ϕ according to the functional form:

$$c_{Pd} = c_{Pd}(\psi, \phi) = f(\psi, \phi) + g(\phi) \tag{5}$$

where $f(\psi, \phi)$ defines the shape of the c_{Pd}-curve and $g(\phi)$ acts as an offset which rigidly shifts the curve up- or downwards, depending on the ϕ value.

To ease the description, the collected dataset is presented in figure 4 without the offset $g(\phi)$, i.e. by directly showing the function $f(\psi, \phi)$, that takes a unity value at $\psi = 0°$ for each pitch angle. The absolute value of yaw ψ is considered on the abscissa, consistently with the setup symmetry for $\pm\psi$ rotations. Contrarily, the probe asymmetry for $\pm\phi$ rotations causes different responses as the pitch varies, and the c_{Pd} curve depends on ϕ through both functions f and g. As regards the offset function $g(\phi)$, its contribution is reported in table 2: a 5% overestimate on c_{Pd} is experienced tilting the probe 5° away from the probe support, effect reduced to less than 1% up to 2.5° rotation in the same direction. Approaching the support causes instead a premature increment in the error module, reaching a 2.7% underestimation at $\phi = +2.5°$. As regards the function $f(\psi, \phi)$, here the pitch ϕ influences the shape of the c_{Pd} curve, but in this case the impact of misalignments in both directions is less critical: regardless of the ϕ value, for yaws $|\psi| < 5°$ this probe design guarantees a dynamic pressure reading within 1% of the reference value. Beyond the $\psi = 5°$ threshold the c_{Pd} curves show specific dependence on the pitch angle and its sign, but preserve a conventional shape and good agreement (error limited to 2%) within $|\psi| < 10°$ for moderate misalignments in a range $-5° \leq \phi \leq 0°$.

Table 2. Offset function $g(\phi)$.

ϕ [°]	$g(\phi)$
-5.0	+0.052
-2.5	+0.006
0.0	0.000
2.5	-0.027

Compared to standard-size popular designs, this probe has a narrower field of alignment where an accurate reading is guaranteed. The possible reasons for this behaviour involve both shape and size of the probe, since for certain orientations the wake of the total head may interact with the subsequent part of the probe, and also the total-head reading becomes increasingly sensitive to misalignments as the size of the Pitot reduces [9].

3.2. Validation on flat plate turbulent boundary layer

To verify the capability of capturing the average velocity profile inside a turbulent BL, the probe and procedure previously described were tested on a canonical flat plate BL, and the readings compared with the information available in literature.

The measurements have been carried out across a BL developed on the tunnel floor relying on the zero pressure gradient of the test section, a setup used in literature as an alternative to a plate immersed in the airstream [3, 7]. For these tests, the tunnel floor is covered with an aluminium plate of thickness 5 mm, with surface roughness of 2 μm rms. The front edge of the plate is joined to the structure with a sandpaper tape. The probe is held above the wall with inclination of 2° as shown in figure 5, to ensure proper contact to the wall at the lowest position as explained in §2.2. The vertical position is set by a traversing system driven by a stepper motor with positioning accuracy of $\pm 7.5\mu$m, and accounting for the tolerances on the probe dimensions the positioning accuracy turns out to be in the order of $\pm 25\mu$m. The vertical sting holding the probe and the traversing unit are mechanically decoupled from the test section frame in order to avoid propagation of vibrations. The sting enters the test section through a hole provided with a bellows. An horizontal translation is possible by manually adjusting the probe position along the s axis shown in figure and combining this with a vertical shift; this allows to follow the procedure of §2.2 for wall measurements, useful in presence of pressure gradients, however preliminary checks confirmed that no changes in static pressure can be revealed in this setup by moving the probe horizontally, so the final measurements have been performed connecting the pressure lines to a single differential transducer. Depending on the airspeed range, two transducers were used, with full ranges of 100 and 500 Pa, both with 0.1% FS accuracy, connected to the same acquisition system described above. Collected data points were corrected for low Re, shear, vicinity to the wall and turbulence effects [1, 3] and carefully validated in close proximity of the surface where the filtering effect caused by the finite area of the tube and measurement uncertainty are more influential.

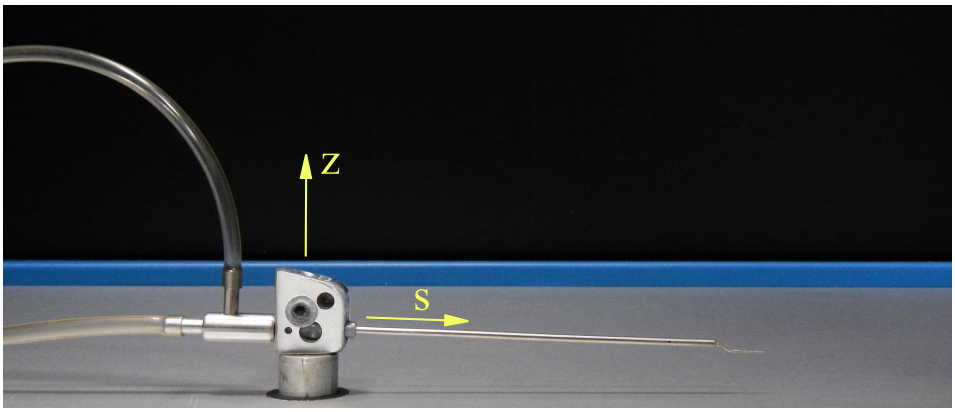

Figure 5. Setup for flat plate BL measurements.

The data were collected at two nominal airspeeds, 10 and 20 m/s, covering the same range as the experiments in which this probe was introduced [4, 5]. The 10 m/s velocity is also the same used for the directional tests above. At the probe location, the BL thickness is well in the operating field of the probe itself, and with the airspeeds above the corresponding Reynolds numbers are Re_θ =1000 and 2500, respectively. The

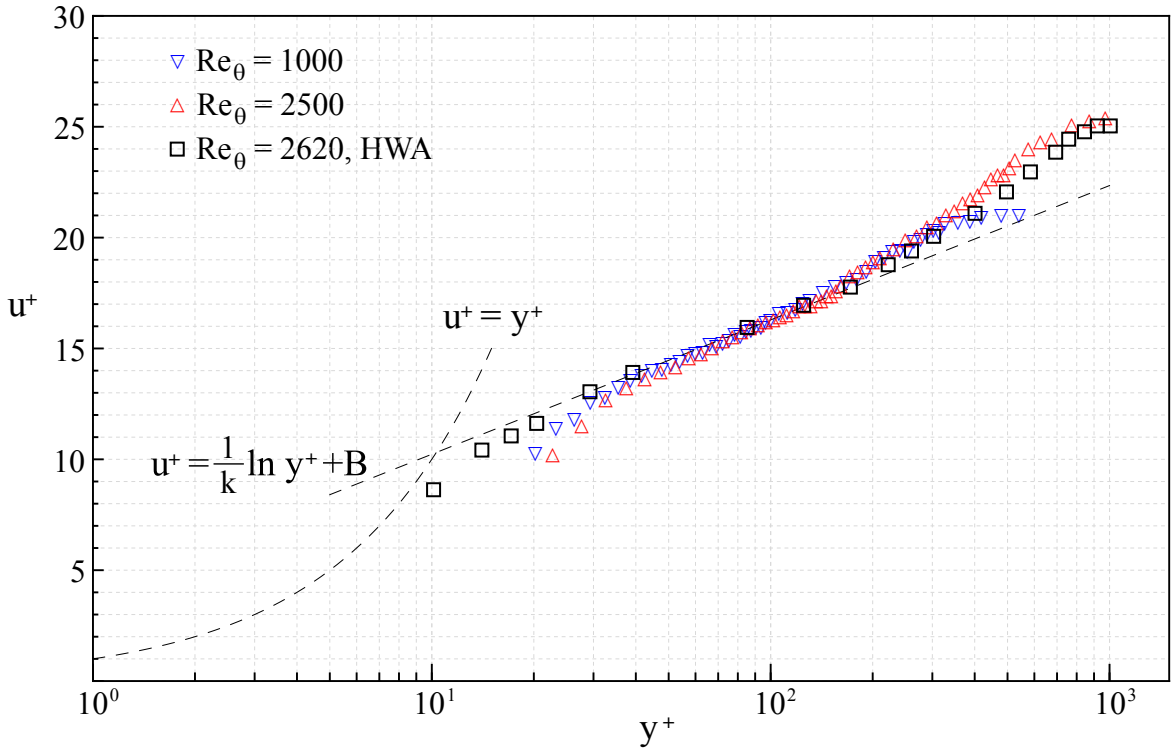

Figure 6. Inner-scaled average velocity profiles. Comparison of two profiles acquired by the present probe at different Reynolds numbers Re_θ and a profile read by a subminiature hot wire probe [11].

shape factors evaluated for these Re_θ are $H = 1.44$ and 1.42, which are typical values for turbulent BL on flat plates, however it is worth to compare the present conditions to the literature data at similar Re_θ. In systems purposely designed to create flat plate turbulent BL, the turbulent conditions are enabled over a wide range of Re_θ, starting from values as low as 1100 [7] or also 500 [8], however in the latter case the shape factor H is 1.57. Also in a comparison of several laboratory and numerical data sets [10] there are turbulent BL data available for low Re_θ, however the relevant shape factors are about 1.4 or lower only when Re_θ is above 1000. Moreover, it is possible to find transitional conditions for Re_θ up to 2000, even if the corresponding H are generally larger than 1.4. The literature survey may suggest $Re_\theta = 2500$ as more appropriate for a fully turbulent velocity profile, however in what follows both the velocity profiles at Re_θ =1000 and 2500 will be presented for completeness. A further turbulent profile with $Re_\theta = 2620$ and $H = 1.41$ has been considered [11] for direct comparison with the present data, as shown below.

Processed data are presented in figure 6, scaling the variables to wall units introduced after determining the friction coefficients from the application of Clauser chart method [12]. The uncertainties, determined by error propagation starting from independently measured quantities, are $\pm 2.5\%$ for y^+ and $\pm 2.2\%$ for u^+. The results present good agreement with the law of the wall, particularly in the $40 < y^+ < 200$

region where the two data sets overlap and closely resemble the logarithmic law

$$u^+ = \frac{1}{k} \ln y^+ + B \tag{6}$$

having assumed coefficients $k = 0.38$ and $B = 4.17$, consistent with the narrow range of values reported in the literature on zero pressure gradient turbulent BL [13]. Figure 6 also shows another profile, obtained on a flat plate BL by means of a subminiature hot wire probe at Re_θ =2620 [11]. This permits a direct comparison with HWA, which is widely used for BL velocities. The present data at Re_θ =2500 are in good agreement with these HWA measurements on the logarithmic region above $y^+ = 40$ and in the upper region, blending with the outer flow. On the other hand, in the buffer region the hot wire probe, whose spatial resolution is better, unavoidably overcomes the Pitot probe.

4. Conclusion

An original pressure probe design has been proposed to ease some kinds of boundary layer measurements, as an alternative to other more sophisticated and/or expensive techniques. A typical application case arises when velocity profiles are needed on a wind tunnel model already built for force measurements and not provided with pressure taps: the present probe can be used to retrieve average velocities in the BL without modifying the model or rebuilding a new version of it. The probe has been efficiently used in this way to retrieve the boundary field over the surface of an airfoil model [4, 5].

In this work, the functionality of the device was thoroughly tested and showed good agreement with well-established results on conventional BL over a flat plate. The sensitivity to flow direction results to be mildly skewed as a consequence of the asymmetry in the nose geometry and with reduced accuracy margins because of the inherent dimensions, effects that can be mitigated by an accurate angular positioning and - under extreme circumstances - compensated referring to a calibration chart incorporated for the operation of the device.

Presented design could be adopted as is for the investigation of boundary layers with thickness in the order of some mm. Thicker boundary layers can also be investigated, provided that the vertical static pressure gradient either remains negligible or can be correctly reconstructed using the static probe. As premised, every other case excessively departing from the one presented here can be treated by a specific analysis, keeping the same design and adapting the probe dimensions to the problem in hand.

References

[1] Tropea C, Yarin A L and Foss J F 2007 *Springer handbook of experimental fluid mechanics* (Springer Science & Business Media)

[2] Buck A L 1981 New equations for computing vapor pressure and enhancement factor *J Appl Meteorol* **20(12)** 1527-1532

[3] Bailey S C C et al 2013, Obtaining accurate mean velocity measurements in high Reynolds number turbulent boundary layers using Pitot tubes *J Fluid Mech* **715** 642–670
[4] Messanelli F, Frigerio E, Tescaroli E and Belan M 2019 Flow separation control by pulsed corona actuators *Exp Therm Fluid Sci* **105**, 123-135
[5] Messanelli F, Frigerio E, Tescaroli E and Belan M 2020 Separation Control by Plasma Actuators: Effects of Direct Momentum Injection and Vortex Generation *Flow Turbul Combust* **104**, 895–926.
[6] East L F, Sawyer W G, "An investigation of the structure of equilibrium turbulent boundary layer," in: AGARD CP-271, Turbulent Boundary Layers - Experiments, Theory and Modelling, The Hague (Netherlands), 1979.
[7] Nickels T B, Marusic I, Hafez S, Hutchins N and Chong M S 2007, Some predictions of the attached eddy model for a high Reynolds number boundary layer *Phil Trans R Soc A* **365** 807–822.
[8] Purtell L P, Klebanoff P S and Buckley F T 1981, Turbulent boundary layer at low Reynolds number *Phys Fluids* **24**, 802–811.
[9] Davies P O A L 1958 The behaviour of a Pitot tube in transverse shear *J Fluid Mech* **3(5)** 441-456
[10] Wei T and Klewicki J 2016 Scaling properties of the mean wall-1 normal velocity in zero pressure gradient boundary layers *Phys Rev Fluids* **1** 082401
[11] Ligrani P M, Bradshaw P 1987 Spatial resolution and measurement of turbulence in the viscous sublayer using subminiature hot-wire probes *Exp in Fluids* **5** 407–417
[12] Clauser F H 1954 Turbulent boundary layers in adverse pressure gradients *J Aero Sci* **21(2)** 91-108
[13] Pope S B 2001 *Turbulent flows* (Cambridge University Press)